ON THE WATER ENHANCED TURBOFAN CONCEPT: PART A - THERMODYNAMICS AND OVERALL ENGINE DESIGN

Alexander Görtz[1], Jannik Häßy[1], Markus Nickl[2], Alexandros Lessis[2], Marc Schmelcher[1] & Mahmoud El-Soueidan[1]

[1]German Aerospace Center (DLR), Linder Höhe, 51147 Cologne, Germany
[2]Bauhaus Luftfahrt e.V., Willy-Messerschmitt-Str. 1, 82024 Taufkirchen, Germany

Abstract

Aviation is responsible for a growing portion of global greenhouse gas emissions contributing to climate change. The Water-Enhanced Turbofan (WET) is a promising concept for reducing the climate impact of aviation in terms of CO2 and Non-CO2 effects. The innovative thermodynamic cycle with a quasi-closed water circuit increases overall efficiency and reduces emissions. However, the Water-Enhanced Turbofan offers a new range of design parameters for the propulsion system. The influence of important cycle parameters such as temperature, pressure and water to air ratio is assessed in this work. Special focus is set on the impact on the WET specific components for the water circuit introduction. Finally, the influence of these changes is evaluated not only at engine level, but also on overall mission fuel burn.

Keywords: Propulsion, Aero Engine, Engine Performance, Water-Enhanced Turbofan

1. Introduction

Aviation is responsible for a considerable portion of global greenhouse gas emissions contributing to climate change. With decarbonization of various private and industrial sectors, the share of aviation is expected to grow continuously if no countermeasures are taken. It is a major challenge to further reduce emissions and the impact of aviation on climate to achieve Europe's ambitious targets [1]. Engine technology plays a major role with respect to emissions, primarily due to the use of kerosene from fossil sources. Evolutionary development of conventional engine architectures remains important but will not enable the required leap to address current challenges. Electric propulsion concepts, fuel cell-based propulsion, drop-in capable Sustainable Aviation Fuels (SAFs) and hydrogen are being researched. However, batteries lack the necessary energy density for long-distance travel. Fuel cell-based propulsion systems do not achieve the high power densities of gas turbines and require an active dissipation of waste heat to the ambience [2]. Synthetic fuel production requires excessive renewable energy as well as infrastructure everywhere around the globe, which is not expected to be available in sufficient quantities in the near future, setting the clear need for highly efficient propulsion systems. The use of hydrogen imposes further challenges with respect to storage, safety, component life and aircraft design.

One promising idea for reducing the climate impact of aviation is the Water-Enhanced Turbofan (WET) proposed by MTU Aero Engines [3]. The WET concept is a gas turbine-based propulsion concept that can run on hydrogen or SAF in addition to kerosene from fossil source and can be used for all aircraft classes. The WET utilizes the residual heat from the engine's exhaust gas to increase thermal efficiency. In terms of the thermodynamic cycle, a Cheng cycle is implemented, which combines the Joule-Brayton cycle with a Clausius-Rankine cycle in parallel execution [4]. Injecting water into the core flow increases the mixture's heat capacity due to the higher heat capacity of water compared to dry air. The higher heat capacity enables the possibility to extract more power from the flow by the

turbines. While this effect is also noticeable for direct hydrogen combustion engines [5], it is even more significant for water injecting gas turbines like the WET. Implementing the Cheng cycle into a gas turbine engine requires the utilization of two additional heat exchangers for evaporation as well as for condensation. The design and the operating behavior of these heat exchangers will be crucial for the success of innovative propulsion systems as the WET [6, 7]. To dispel these uncertainties, demonstrations of the WET system will be carried out [8, 9]. While the water loading of the air in conventional aero engines is rather low and mostly due to humidity of the ambient air or rain, it is not necessary to use gas models with a high water fraction in the performance analysis. This changes for the WET as the water loading is the main driving force for this innovative concept. A gas model with water to air ratios of up to 40 % has to be assessed and validated prior to the cycle analysis [10]. This implementation of an additional water circuit in the engine leads to a decrease in thrust specific fuel consumption and carbon dioxide (CO2) emission. Furthermore, the WET has the potential to also reduce the non-CO2 effects that contribute to global warming: First, the injection of water lowers the amount of nitrogen oxides produced during combustion. Second, the WET concept may reduce contrail formation [11, 12]. While the reduction of CO2 emissions is mainly defined by the overall fuel consumption the climate impact of non-CO2 effects outweigh those of CO2 anyway [13, 14] increasing the potential of a WET towards climate neutral aviation. A further decrease of climate impact of the WET is possible by using hydrogen as fuel, eliminating direct CO2 emissions completely from the engine. Using hydrogen has the additional benefits of synergies between the WET and hydrogen's specific properties. Burning hydrogen produces 2.8 times more water than kerosene for same energy delivery increasing the effect of a higher heat capacity after combustion even more [15]. In addition, hydrogen will be stored as a liquid at 20 K in the aircraft's fuselage but has to be heated up before combustion. This conditioning process can be used as a heat sink for the condenser in a WET reducing its size and weight [16]. Parametric cycle studies of the WET with kerosene have already been presented by Ziegler et al [17] targeting a minimal thrust specific fuel consumption as well as a minimal overall fuel burn for a variety of design values. However, in this study simplifications e.g. constant turbomachinery efficiency and constant stage numbers were made.

This work investigates the design space of a specific WET architecture with respect to the thrust specific fuel consumption, weight and the overall fuel burn. In addition to typical turbofan design variables like overall pressure ratio, turbine entry temperature and bypass ratio, this work also focuses on WET specific design parameters. The thermodynamic cycle calculation is extended in such a way that the geometry of the turbo components and the heat exchangers is generated. This geometry is used to estimate masses and in the case of turbomachinery also the corresponding efficiencies. This paper will answer the following research questions:

- What is the impact of Overall Pressure Ratio (OPR), Turbine Entry Temperature (T4), Water to Air Ratio (WAR) after steam injection and further design values on WET propulsion system design and performance?
- How does a variation of these parameters affect the WET specific components?
- What is the best combination of parameters considering the overall mission fuel burn?

This work (Part A) is complementary to the paper "ON THE WATER ENHANCED TURBOFAN CONCEPT: Part B – Flow Path and Mass Assessment" [18]. Part B focuses on the turbomachinery geometry, flow paths and overall mass estimation. Thermodynamic cycle data from part A is the basis for the flow path and mass investigations presented in Part B. The results are fed back to Part A to estimate overall system performance including penalties related to dimensions and mass.

2. Water Enhanced Turbofan

The Water Enhanced Turbofan concept itself is not defined by a specific architecture. Many arrangements and additional components are conceivable while the main features as steam injection, evaporation and condensation will remain. However, for this work a specific architecture is selected and kept constant throughout all conducted studies. The corresponding architecture is shown in the engine

model scheme in Figure 1. The geared turbofan consists of two spools but without a booster compressor as the overall pressure ratio is rather low compared to conventional aero engines, whereby an additional compressor would become unnecessary. The previously evaporated water is injected after the last high pressure compressor (HPC) stage in the form of steam. The combustion takes place with a highly water loaded air resulting in comparatively high fuel to air ratios. However, a high fuel to air ratio does not imply higher temperatures because the core flow has a higher heat capacity after steam injection. Both turbines, the high pressure turbine (HPT) and the low pressure turbine (LPT), are cooled. While the LPT is cooled with dry air from the HPC, the HPT is cooled using water loaded air after the steaminjector. This is beneficial as this air has higher potential of heat removal due to its higher heat capacity. The evaporator (Heat Recovery Steam Generator - HRSG) follows the turbine section with the core flow on the hot side and liquid water on the cold side. The water is evaporated and super heated, providing steam for further use. The already cooled but not yet condensed exhaust core flow then enters the condenser. The core flow is cooled further at this point, so that water begins to condense. Part of the bypass flow serves as a heat sink here. In order to minimize the pressure loss in the bypass, only part of this flow is guided through the condenser. The water formed during condensation will be separated from the main flow after the condenser. After separation the water's pressure is increased by a pump before entering the evaporator. Increasing the pressure of the water side at this position is beneficial as increasing the pressure of a liquid requires less energy than increasing the pressure of a gas such as steam. The water has to be pressurized because it will be injected into the core flow after the HPC. Therefore, a pressure of the water side higher than p_3 is necessary. The superheated steam is going to have a temperature similar to turbine outlet temperatures. Increasing the water's pressure even more enables the possibility to add a steam turbine after the evaporators outlet. This turbine is supporting the low pressure shaft while ensuring a pressure of the steam still higher than p_3 for injection. Overall, this allows a closed water circuit to be integrated into the engine.

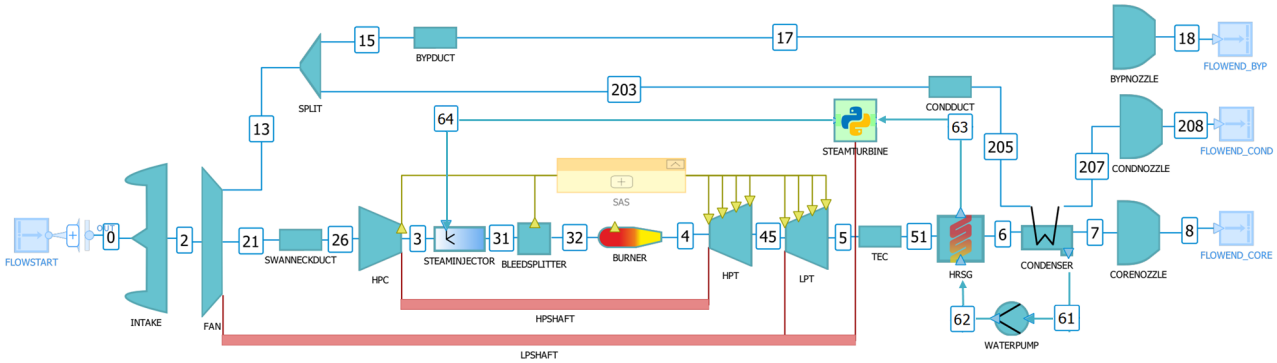

Figure 1 – Engine Model Scheme

3. Aircraft Design For An Application With A Water Enhanced Turbofan

To set an appropriate engine design target, the influence of varying engine parameters on the aircraft performance needs to be considered. Therefore, a reference aircraft equipped with the WET is designed. This model can then be utilized to derive linear trade factors on parameters of interest which can be used during the engine design process.

3.1 Aircraft Design Methods

To conduct all aircraft modelling, the Bauhaus Luftfahrt Aircraft Design Environment (BLADE) is employed. A detailed explanation of the overall BLADE aircraft design methodology and subsequent aircraft derivatives can be found in [19]. BLADE primarily employs semi-empirical methods for aircraft sizing, focusing on mass estimation, aerodynamics, overall aircraft performance and the equations of motion [19, 20, 21, 22], and is designed to interact with a CPACS (Common Parametric Aircraft Configuration Schema [23]) representation of the aircraft. Furthermore, a sophisticated scaling approach is applied to derive the WET engine performance from a reference data set. This scaling considers

the WET engine characteristics along the entire design mission trajectory. Therefore, all relevant assumptions and parameters are reflected within the model and allow the derivation of sensitivities for certain aspects of the design.

In addition to the conventional aircraft modelling, WET-specific considerations are also accounted for. In particular, a single water storage tank is placed in the cargo compartments of the aircraft, similarly to the additional center fuel tanks, and the mass of itself and its systems is modelled. The water tank mass is derived from a linear regression based on commercially available polyethylene tanks, relating its volume to its mass. As for the tank systems - pumps, service panels, plumbing, valves and wiring are considered and their mass is fixed to 222kg based on [24]. The water tank centre of gravity (CG) is located on its volumetric centroid, whereas the systems CG is placed on the aircraft's operating empty mass (OEM) CG.

The aircraft linear trade factors are derived from high-level engine parameter variations that have a direct effect on the aircraft performance. Particularly, to account for engine design variations, aircraft designs with a different specific fuel consumption, fan diameter, nacelle length and engine mass are generated. Each of the aforementioned individual parameter variations results in a new aircraft design according to the employed sizing strategy. The relative changes in typical mission kerosene fuel burns define the trade factors connected to each parameter variation.

During the aircraft sizing process, the wing loading, static margin and empennage stability volume coefficients are kept constant as the aircraft's mass and aerodynamic characteristics are calculated. The engine design point is fixed at the top of climb (TOC) mission point, whereas the design point thrust level is determined based on several requirements. Specifically, target values for the time to climb, TOC specific excess power, takeoff field length and second segment climb gradient are set and the most constraining one is selected to calculate the aircraft's design thrust.

Regarding the WET-equipped aircraft, certain operational strategies need to be defined. Depending on the ambient conditions and thrust demand, additional water needs to be supplied to the engine from the airframe. This is referred to as "external water" and for the purposes of this study it is supplied only for the takeoff and climb segments of each mission. Moreover, to ensure that sufficient external water is carried on board for each mission, an additional mission that maximizes this external water demand is analyzed, as shown in Figure 2. It is identical to the design mission, however, no cruise segment is performed and the aircraft mass during diversion is much higher, thus increasing the external water demand during go-around and diversion climb. Therefore, this mission defines an additional water mass that needs to be carried throughout all other missions and is not consumed. Furthermore, to offset the penalties associated with carrying the external water on board, specific operational variations can be employed. In particular, the climb schedule speeds can be lowered to reduce the climb thrust demand, which applies to both trip and diversion climb. Additionally, the external water required for diversion is carried throughout the entire trip segments of the mission and therefore has a large influence on the aircraft performance. Thus, a lower diversion cruise altitude can be adopted to reduce this impact. Finally, to decrease the thrust demand for segments requiring an external water supply (takeoff and climb), the engines can be derated, as long as no top level aircraft requirement is violated.

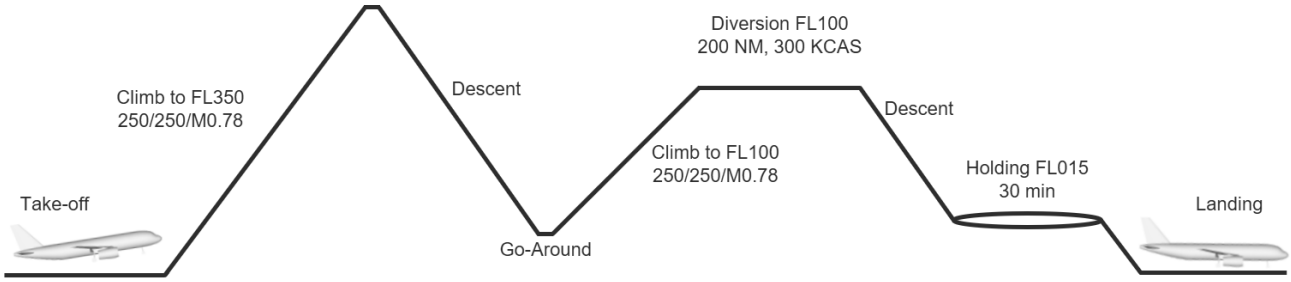

Figure 2 – Mission profile of additional no-cruise mission.

3.2 Reference Aircraft

A medium range class aircraft is selected for this study. It is equipped with a WET engine and several technological improvements are applied considering an entry into service in 2035. These improvements include lighter structures through the use of composite materials, all-electric subsystems that remove the need for hydraulic systems and a high performance wing with higher aspect ratio and foldable wingtips to comply with airport compatibility regulations. An overview of the resulting reference aircraft data is shown in Table 1 and an isometric view of its geometry is illustrated in Figure 3. It should also be noted that the focus of this paper is around the engine design rather than the aircraft and therefore further investigations need to be conducted to assess the effect of additional variations that can benefit the aircraft's performance.

Table 1 – Reference aircraft data.

	Value	Units
Design Range	3000	NM
Cruise Mach	0.78	-
Cruise Altitude	35000	ft
Time to climb	25	min
Takeoff field length	2400	m
Second segment climb gradient	2.4	%
TOC specific excess power	580	ft/min
Maximum takeoff mass	85.39	t
Engine mass	5.58	t
Wing area	134.0	m^2
Design thrust at TOC, per engine	25.6	kN
Lift to drag ratio, mid-cruise	18.6	-

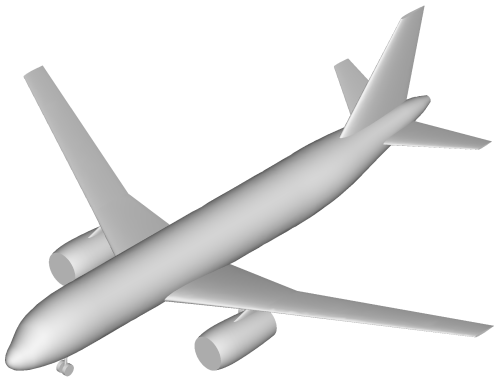

Figure 3 – Reference aircraft.

A design block range of 3000NM at Mach 0.78 is selected and the operational strategies described in 3.1 are employed. Despite the larger nacelles and the heavier maximum takeoff mass, a high lift-to-drag ratio is achievable, which is mainly attributed to the high performance wing. Based on the predefined engine sizing requirements, the top of climb specific excess power is the most constraining one and thus is used to size the engine. Table 2 shows the engine non-derated thrust requirements at takeoff, top of climb and mid-cruise, all of which are necessary for the engine design process, as described in 4. It should be highlighted that the TOC specific excess power requirement is set to a rather high value and future iterations of this aircraft should assess its effect on the resulting aircraft performance. Although the required thrust level and thus engine size are similar to equivalent state-of-the-art aircraft applications, the engine mass increases significantly due to heat exchangers and other WET specific propulsion system components. The nacelle length is also increased to house the concept specific components, which adds additional weight to the total engine mass.

Table 2 – Engine spot point thrust requirements at design mission.

	Units	Takeoff	Top of climb	Mid-cruise
Altitude	ft	0	35000	35000
Mach	-	0.00	0.78	0.78
ISA deviation	K	+15	+10	0
Thrust, per engine	kN	153.2	25.6	20.0

Based on this aircraft design process, parameter studies are performed to derive the aforementioned trade factors that are defined in 3.1. For each engine parameter variation, a new aircraft is designed for the same design mission, and their effects on the fuel burn on a typical mission are reported in Table 3. The impact on the typical mission is chosen as this is a more representative mission for the operation of the aircraft. It is similar to the design mission with the exception of a block range

reduction to 800NM and all segments being simulated at ISA conditions.

Table 3 – Relative block fuel burn differences at typical mission.

	Parameter variation	Fuel burn variation
Specific fuel consumption	+1 %	+1.260 %
Engine mass, per engine	+500 kg	+1.990 %
Fan diameter	+10 cm	+0.507 %
Nacelle length	+10 cm	+0.169 %

4. Engine Design

The engine design process can be divided into two sections. The first being the thermodynamic cycle analysis and secondly the geometry generation combined with mass assessment and turbomachinery efficiency calculation. The multidisciplinary virtual engine platform *GTlab* is used to combine all disciplines into one design procedure [25]. This highly iterative process requires on the one hand an exchange of performance data towards the geometry generation and on the other hand turbomachinery efficiency as well as engine weight towards the thermodynamic analysis. This process is described by Häßy et. al in detail [26, 27] but is applied to a Water-Enhanced Turbofan for the first time in this paper.

4.1 Engine Performance

The engine performance calculation is carried out using the DLR internal performance program *DLRp2* which is integrated into *GTlab* [28]. A picture of the corresponding engine architecture is shown in Figure 1. The iteration scheme is presented in Table 4. For the design process either the fan diameter or the bypass ratio can be defined as input. In case of the reference engine a value for the fan diameter similar to the PW1100G engine diameter is selected whereby the bypass ratio results from this condition. However, the following design studies will have a constant bypass ratio or it will be mentioned otherwise, see Chapter 5. Selecting the optimal fan pressure ratio of the bypass flow regarding minimal fuel consumption for a conventional turbofan engine is often done by reaching an ideal nozzle velocity ratio [29]. While this approach has been proven to be valid for a turbofan, it is not applicable for a Water-Enhanced Turbofan. Removing heat from the core flow and decreasing its temperature results in different flow conditions and speeds of sound at the core nozzle, invalidating this condition for this type of engine. A nozzle velocity ratio of > 1 has proven to achieve lower thrust specific fuel consumption leading to a faster bypass nozzle flow velocity compared to the core nozzle flow velocity. Grieb [30] presents information available for the fan tip velocity of existing turbofan engines and therefore providing a correlation between fan pressure ratio and fan rotational speed. While the low pressure spool speed is determined by the low pressure turbine, see Section 4.2, the fan rotational speed is defined by the gear ratio of the fan. This gear ratio can be calculated with the provided correlation from Grieb and the low pressure spool speed. While the pressure ratio of the core part of the fan is kept constant for simplification, the overall pressure ratio is only defined by the pressure ratio of the high pressure compressor since no booster compressor is available. The power of the steam turbine also depends on the overall pressure ratio since a steam injection pressure of 5 bar higher than p_3 is selected while keeping the water pressure prior to the evaporator constant. The required amount of turbine cooling air is estimated with a simple approach using Grieb [30] but with an adaption regarding the heat capacity of the core flow and the cooling air.

While the conventional components in an engine are modeled using common models for engine performance calculations, the WET-specific heat exchangers are modelled using their temperature profiles in Figure 4 and 5. The evaporator can be divided into 3 segments as follows: preheating, evaporation and superheating. Both flow inlet conditions are known during the engine design process. The entire temperature profile is defined if either the transferred heat or one outlet temperature or rather temperature difference is given. For this work a minimal temperature difference dT_{min} is used. This temperature difference can either occur where the water enters the two phase segment

Table 4 – Iteration Scheme for Engine Design

Independents	**Dependents**		
Cruise	LHS	RHS	Unit
Fan Pressure Ratio	Nozzle Velocity Ratio	1.1	[-]
Bypass Ratio	Fan Diameter	2.05	[m]
Gear Ratio	Fan Tip Speed	Fan Tip Speed Grieb	[m/s]
HPC Pressure Ratio	Overall Pressure Ratio	30	[-]
Water to Air Ratio	dT_Mid	dT_Out	[K]
Fuel to Air Ratio	Turbine Entry Temperature	1600	[K]
Massflow	Thrust	20	[kN]
Steamturbine Power	Steam Pressure Injection	p3 + 5 bar	[bar]
Cooling Air	WQW	WQW_Grieb	[-]
Maximum Take Off	LHS	RHS	Unit
Fuel to Air Ratio	Thrust	153.2	[kN]
Water to Air Ratio	Turbine Entry Temperature	1875	[-]
Top of Climb	LHS	RHS	Unit
Fuel to Air Ratio	Thrust	25.6	[kN]
Water to Air Ratio	Turbine Entry Temperature	1720	[-]

between I and II dT_{mid} or at the overall outlet of the heat exchanger dT_{out}. In addition, the ratio between the core mass flow and the water mass flow is defined by the water to air ratio at steam injection. It has been found that the lowest thrust specific fuel consumption results if both temperature difference are identical $dT_{mid} = dT_{out} = dT_{min}$. For a specific minimal temperature difference, the water to air ratio can be varied to fulfil the best temperature distribution. The methods used in the surrogate model for off design calculation are presented by Nöske [31] and a direct comparison of this surrogate model to a tool of a higher order was done by Schmelcher et al. [7]. The pressure losses of the evaporator are modeled with a linear function depending on the flow length.

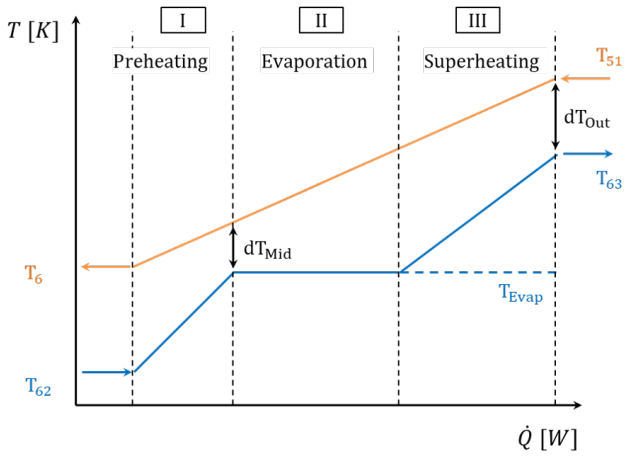

Figure 4 – Evaporator Model

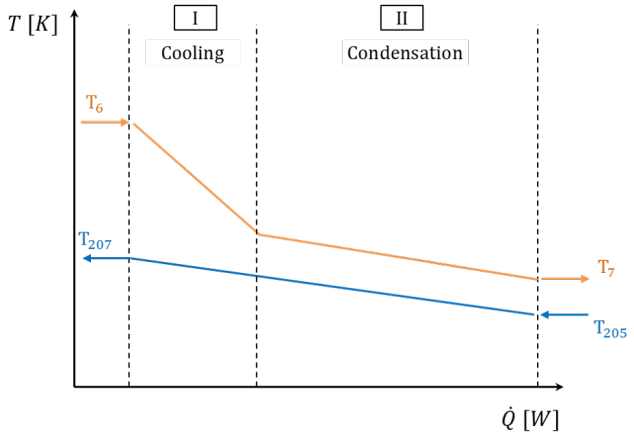

Figure 5 – Condenser Model

Similar to the evaporator, the condenser inlet conditions of both flows are known during design. The core inlet flow is steam loaded wet air while the heat sink is dry air coming directly from the fan bypass flow. The condenser is divided in two segments. The first segments' purpose being cooling the core flow until the temperature of condensation is reached. At this temperature the first water droplets begin to form and condense from the steam loaded air. To this point the heat exchanger is modelled as a plate heat exchanger with gas on both sides. The simplified correlations for heat transfer coefficients of a even plate are used for this segment [32]. The second segment is the

condensation itself with dry air on the side of the heat sink and wet air on the other side combined with a liquid phase. The pressure losses of the condenser are modeled with a linear function depending on the flow length. To calculate the outlet temperature of the core flow, new values are introduces. The overall water recovery factor WRF Equation 1 and the injection specific water recovery factor $WRF^{\star}$ Equation 2.

$$WRF = \frac{W_{Water,Recovered}}{W_{Water,Available}} \tag{1}$$

$$WRF^{\star} = \frac{W_{Water,Recovered}}{W_{Water,Injected}} \tag{2}$$

The mass flow of recovered water $W_{Water,Recovered}$ is the amount of water that is separated from the main flow and which will be fed back to water circuit. In the engine model scheme Figure 1 this would be the station 61. The available water mass flow $W_{Water,Available}$ is the sum of all water in every physical state in the flow; including the amount injected at the steaminjector $W_{Water,Injected}$ and the amount of water due to combustion of kerosene. For cruise operation a closed water circuit is required leading to a $WRF^{\star} = 1$. All previous injected water has to be separated to fulfil this condition leaving only the water due to combustion in the flow. Therefore, a $WRF^{\star} = 1$ directly defines the outlet temperature T_7 because a relative humidity of 100 % can be assumed under this conditions. The heat transfer coefficients for the second segment on the condensation side have been modelled using correlations from Garcia et al. [33]. A further difference to a conventional turbofan is the possibility to adjust the turbine entry temperature for each operating point individually more or less independently from the design point. Therefore, two solutions exist to achieve the same thrust by either changing the amount of fuel burned or by changing the amount of water injected. To handle this characteristic, the turbine entry temperature for maximum take off, top of climb and cruise are set to a fixed value reducing the possible solutions to one.

4.2 Geometry and Turbo Machinery Efficiencies

The generation of the engines geometry and the calculation of turbo machinery efficiency is a highly iterative process and is described in detail in Part B of this work [18]. First, the thermodynamic cycle is calculated using the iteration scheme in Section 4.1 . Based on the resulting data, the flow path of the turbo machinery is created as well as the WET specific components and further necessary additions due to the new engine concept. The flow path analysis and a selection of materials makes it possible to calculate the weight and mechanical stresses of each component. The efficiencies of the turbo machinery are also calculated at this point and fed back to the thermodynamic model. A fixed point iteration is applied until the change in turbo machinery efficiency is below a certain tolerance and a limit regarding circumferential speed or disk loading is reached. Whilst the weight and overall dimensions of the engine itself have no direct effect on the thermodynamics, the impact on mission fuel consumption can be assessed.

4.3 Reference Engine

The reference engine is the result of the overall engine design from the thermodynamic iteration scheme in Section 4.1and the flow path analysis combined with efficiency iteration in Section 4.2. A full mass breakdown of the components is done in Part B of this work [18]. The main performance data are presented in Table 5.

In addition to the performance data, the 2D geometry of the reference WET-engine is presented in Figure 6. For a fixed fan diameter, which was selected based on current engines for this thrust class, the bypass ratio of 21.8 of the WET is significantly higher. This is due to the increase working capability of the core engine. The compressor inlet mass flow is reduced because the mass flow of the turbines is increased with the additional steam injected. Therefore, the turbines have to provide less power for the compression of the core flow and the higher heat capacity of the water loaded flow allows to extract more work. Hence, more mechanical power is available for thrust generation of the fan which is realized with a higher bypass mass flow and therefore higher bypass ratio. The overall pressure ratio of 30 is mainly limited by the blade height of the last high pressure compressor stage.

Table 5 – Reference Engine Cycle Data

Parameter	Unit	Cruise	Take-Off	Top of Climb
BPR	-	21.8	19.5	20.2
OPR	-	30	31.7	35.6
T4	K	1600	1875	1720
Fan Diameter	m	2.05	2.05	2.05
dT_{min}	K	30.0	40.7	37.4
WAR	-	0.123	0.158	0.161

Because of the high bypass ratio the core engine gets smaller resulting in annulus heights below 10.5 mm. This constraint can possibly be relaxed by the use of an axial-radial HPC, which was not considered in this study. The value for a minimal temperature difference $dT_{min} = 30\ K$ of the evaporator was selected in a way that over the whole temperature profile a large temperature difference between both sides is available, leading to small HEX surface areas, while ensuring a large amount of overall heat transfer. The water to air ratio of $WAR = 0.123$ is adjusted as the condition of $dT_{mid} = dT_{Out}$ has to be satisfied.

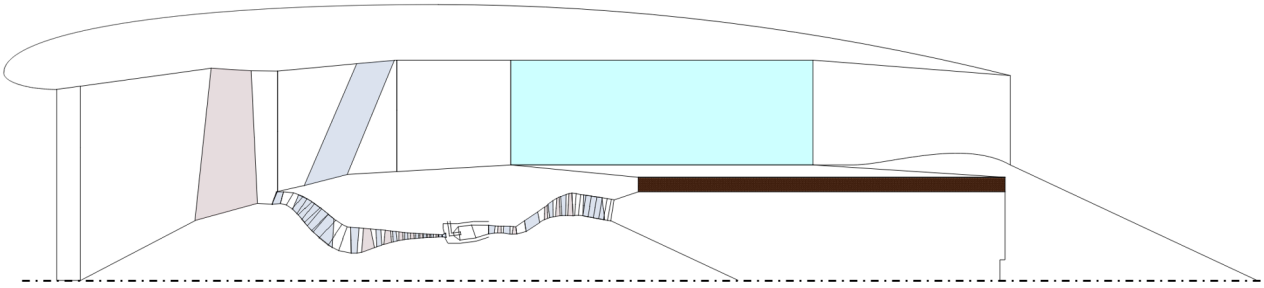

Figure 6 – Reference WET-Engine Design

5. Parameter Studies

For the parametric studies presented in this section, the main design process from Chapter 4. is carried out for each sample. The only difference being that the fan diameter is not a constant value anymore because keeping a constant bypass ratio is a better value to ensure comparability during the study. In addition, the turbine entry temperature at maximum take-off is also removed from the equation system, but is replaced by a constant $WRF^{\star}$ at this operating point, so that there is only one possible solution for this operating point. For each conducted study, the focus was set on two sets of values. First of all, the overall mission fuel burn and the corresponding parameters which were selected in Table 3 and Equation 3.

$$\Delta FB = \frac{\partial FB}{\partial TSFC} \cdot \frac{TSFC - TSFC_{Ref}}{TSFC} \cdot 100\% + \frac{\partial FB}{\partial m} \cdot \frac{(m - m_{Ref})}{500\ kg} + \frac{\partial FB}{\partial D} \cdot \frac{(D - D_{Ref})}{10\ cm} + \frac{\partial FB}{\partial l} \cdot \frac{(l - l_{Ref})}{10\ cm} \quad (3)$$

Secondly, the main WET-specific values on cycle analysis level. Transferred heat of the heat exchangers, power of the steam turbine and water to air ratio were selected. The first two studies, for overall pressure ratio and bypass ratio, are analysed in depth in Part B [18] with regard to the engines mass breakdown.

5.1 Overall Pressure Ratio

The results of the OPR study are presented in the Figures 7 and 8 for a range of $24 < OPR < 37$. The overall difference in mission fuel burn decreases with higher OPR from + 7 % to - 2 % for the selected boundaries. With increasing OPR, the pressure level gets higher but less specific power is

provided by the core. Therefore, the mass flow through the core has to increase to provide enough power for the fan. While keeping the BPR constant, this conditions leads to a higher fan diameter and lower fan pressure ratio for higher OPRs. A higher pressure level also increases the thermal efficiency of the cycle and thus leading to lower TSFC. For a constant turbine entry temperature the optimal OPR for the lowest TSFC is outside of the selected parameter range $OPR > 37$. For a low OPR the condenser determines the engines length by a significant portion. Even tough the fan diameter increases, therefore also the core engine length, the overall engine length decreases as the condenser becomes smaller with higher OPR. This trend changes at around $OPR = 30$ as the impact of condenser length becomes smaller until the core engine determines the engines length. Between OPR 33 and 34 an additional stage is needed in the HPC resulting in a jump in engine length. The number of stages increases from 8 to 9 at this pressure ratio. As the engine gets more compact for higher OPRs and the condenser becomes shorter and lighter, the WET Engine Mass decreases. The additional stage of the HPC has also an effect on the engine weight. Higher OPRs lead to lower turbine outlet temperatures. This results in a different material selection for parts of the LPT and thus in a jump in engine mass from 36 to 37. While increasing the OPR, the blade height of the last stage of the HPC decreases. The reference engine already has a annulus height of 10.5 mm at the compressor outlet which is already ambitiously small.

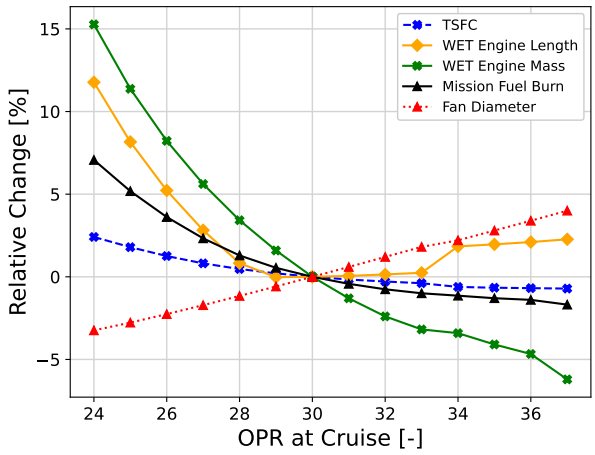

Figure 7 – Mission Fuel Burn

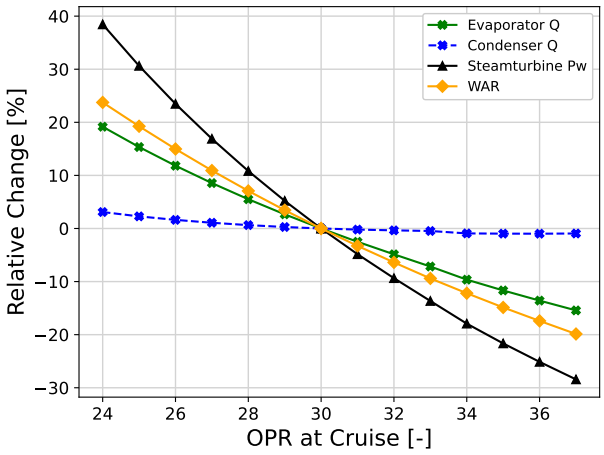

Figure 8 – WET Specifics

The lower turbine outlet temperature also leads to lower evaporator entry temperatures and therefore less available heat for the evaporation of water. Less heat means that less water can be evaporated resulting in less water being injected and reducing the WAR. A lower water mass flow directly reduces the power the steam turbine can provide. This also leads to higher inlet temperatures in the condenser reducing its size. In addition, a higher p_3 requires a higher pressure of the steam at the injection point and therefore reducing the pressure ratio of the steam turbine towards even lower power.

5.2 Bypass Ratio

The results of the BPR study are presented in the Figures 9 and 10 for a range of $19 < BPR < 28$. The overall difference in mission fuel burn decreases with higher BPR from + 12 % to - 4 %. The fan diameter increases significantly with the BPR in a linear way. A higher fan diameter leads to a higher mass flow through the engine and therefore lower specific thrust. This on the other hand means the propulsive efficiency increases, reducing the thrust specific fuel consumption. This reduction of TSFC starts to flatten for the higher BPRs. While the TSFC has a major contribution to overall mission fuel burn, engine size and weight starts to take over. As the fan diameter gets larger the engine gets longer as well. The first kink in engine length between BPR 21 and 22 is due to the absolute lengths of the evaporator and the condenser. For higher BPR the evaporator gets longer than the condenser and starts to determine the length of the WET system and therefore the overall engine length. Long

heat exchangers also lead to higher pressure losses and thus increasing the TSFC for small BPRs. Additionally as the fan diameter increases also the core engines length increases and thus the whole engine becomes larger. Regarding the engines mass, two opposing trends begin to occur. The turbo machinery gets heavier as the engine gets larger with BPR but the WET system becomes smaller.

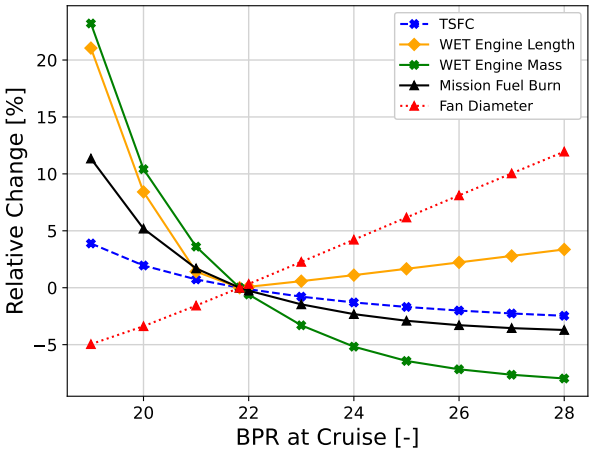

Figure 9 – Mission Fuel Burn

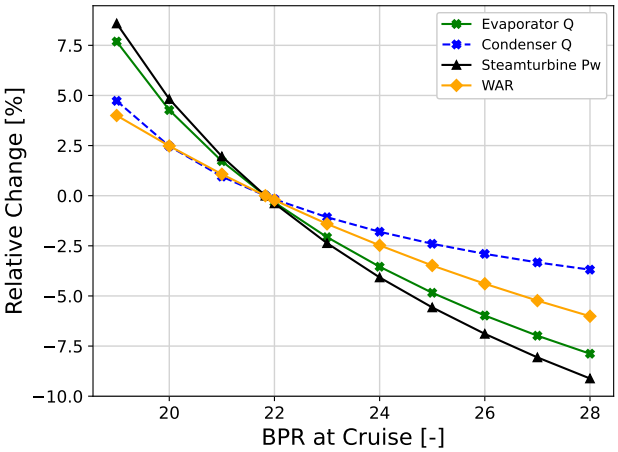

Figure 10 – WET Specifics

For higher BPR the fan pressure ratio gets lower resulting in lower flow velocities at the bypass nozzle. While a constant nozzle velocity ratio is demanded, the velocity of the core nozzle has to decrease as well. This is achieved by a lower pressure for the core flow with the turbines expanding more. A lower pressure after the LPT also means a lower temperature and therefore less heat available for evaporation. Requiring the same temperature differences in the evaporator then leads to less water being evaporated and thus reducing the WAR. Lower water mass flows directly impact the amount of heat transferred within the heat exchangers and less power being provides by the steam turbine.

5.3 Turbine Entry Temperature

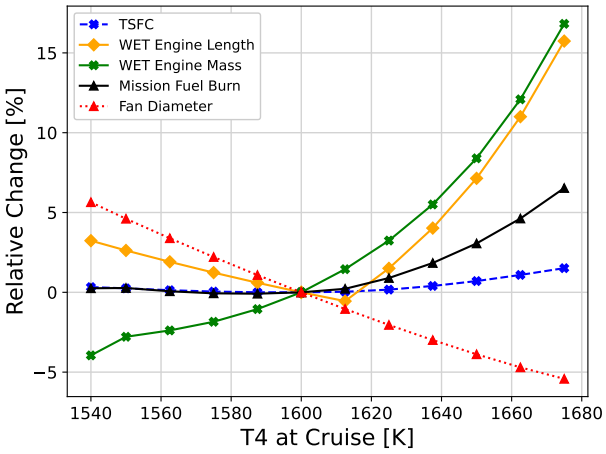

Figure 11 – Mission Fuel Burn

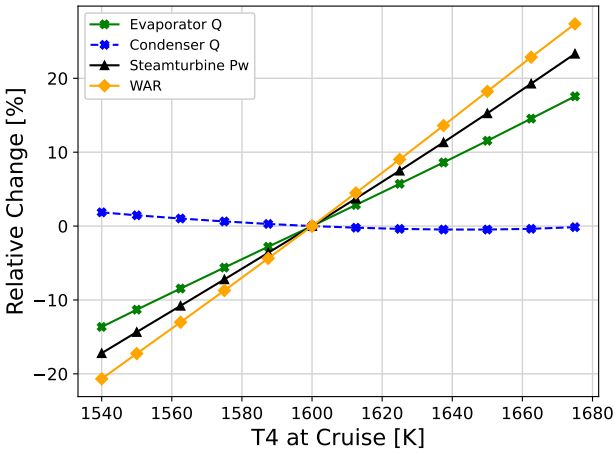

Figure 12 – WET Specifics

The results of the T4 study are presented in the Figures 11 and 12 for a range of $1540\ K < T4 < 1680\ K$. The overall difference in mission fuel burn ranges with T4 from 0 % to + 5.5 % where a minimal mission fuel burn is reached just below $T4 = 1600\ K$. The fan diameter decreases with higher T4 because the core engine gets more effective providing more specific power. For a constant OPR, as assured during this study, the best T4 in terms of TSFC is reached close to the reference point at $T4 = 1600\ K$ as the differences in this area are quite small. For the engine mass two effects occur that

tend to lead in different directions. A lower fan diameter leads to smaller and lighter turbo machinery whereas the mass of the WET system increases. A step in engine mass can be seen between 1540 K and 1550 K since a heavier material for the last LPT disk has to be used since the temperatures in the turbine section increases. Hand in hand with the fan diameter, the engine length decreases as the mass flows decreases. Starting at 1610 K, the WET system gets more impact on the engine length as the condenser mainly determines the overall length at this point.

Higher temperatures at the turbine entry also lead to higher temperatures after the LPT. This results in more thermal energy being available at the evaporators entry and thus leading to higher WARs. Higher water mass flows are the reason for more heat transfer for the evaporator and more power of the steam turbine. In addition, higher heat transfer at evaporation results in lower temperatures of the core flow at the condenser inlet, thus reducing its required transferred heat. Unfortunately, this also leads to lower temperature differences within the condenser and thus increasing its length and mass.

5.4 Water to Air Ratio

The results of the WAR study are presented in the Figures 13 to 16 for a range of $0.09 < WAR < 0.16$. The overall difference in mission fuel burn varies for the WAR from + 7 % to - 0.1 % and the overall minimal fuel burn is close to the reference point and for smaller WAR. This is because the impact of TSFC on the mission fuel burn is comparatively high and the claim during the design process $dT_{mid} = dT_{out}$ already leads to the lowest TSFC for a specific WAR. This condition means that the highest heat transfer per water mass flow is achieved and thus the highest potential to increase the efficiency of the cycle is possible. The condition of same temperature differences within the evaporator no longer works in this study. Therefore, the location of the minimal temperature difference dT_{min} changes. Lower WARs leading to the minimal temperature difference being at the evaporators outlet and higher WARs leading to the minimal temperature difference being at the entry into the two phase regime of the water. Increasing the WAR implies higher water mass flows and thus higher mass flow in the turbines compared to the mass flow through the compressors. Therefore, less air is necessary for the core engine and by keeping the BPR constant the fan diameter decreases as the engine gets more compact. This compactness is also visible by looking at the engines length over the course of higher WARs. The kink between WAR of 0.13 and 0.135 is again due to the change of which heat exchanger is determining the engines length. The course of difference in engine mass is dominated by the mass of the heat exchangers as those components changes the most by increasing the WAR. The kink in engine mass at the reference point is due to the evaporator becoming smaller as the mass flow decreases but the transferred heat is increasing.

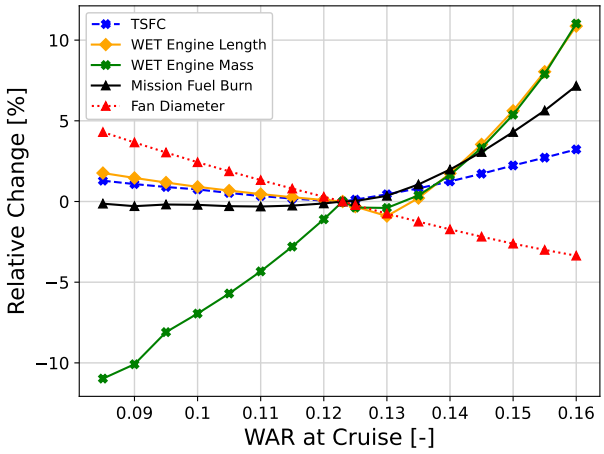

Figure 13 – Mission Fuel Burn

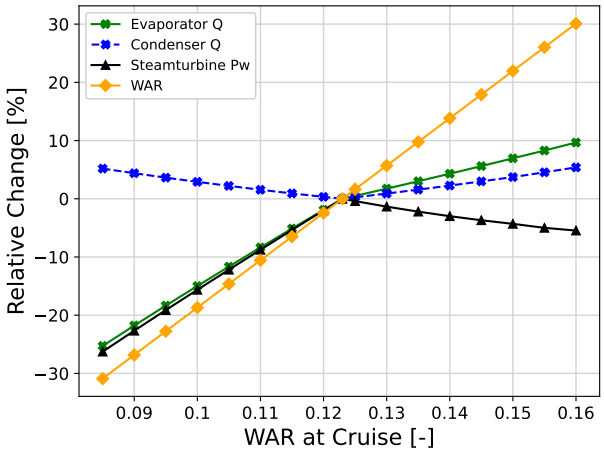

Figure 14 – WET Specifics

Higher water mass flows leads to more heat transfer in the evaporator. The gradient of this values changes as the position of the minimal temperature difference switches towards the entry into the

two phase segment. If this happens, the steam temperature at the outlet will decrease and there is less energy in the steam available which the steam turbine could extract and thus reducing its power output. During the switch, not only the steam gets colder but also the core flow would not be cooled as much as before. Therefore, the condenser has to transfer more heat after switch of the minimal temperature difference location. Since the HPT is cooled with steam loaded air, the cooling capability increases reducing the demand of cooling air. While the condenser gets steadily larger as more water is added the evaporator behaves different as the WAR of the reference engine is reached. As this point is reached and the outlet temperature of the steam gets colder, the overall temperature difference between exhaust and water/steam gets larger reducing the evaporators transfer area and thus its thickness.

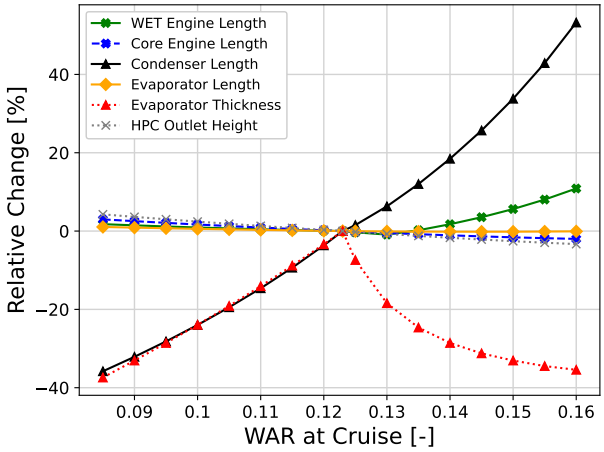

Figure 15 – WET Sketching

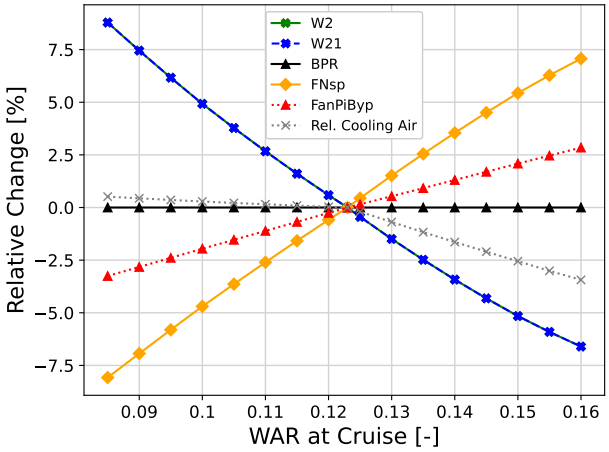

Figure 16 – Overall Data

5.5 Nozzle Speed Ratio

The results of the nozzle speed ratio study are presented in the Figures 17 and 18 for a range of $0.9 < SpeedRatio < 1.2$. The overall difference in mission fuel burn decreases with higher speed ratios from + 2 % to 0 % with a minimum close to the reference engine at $SR = 1.1$. A higher speed ratio can be either achieved by higher pressure at the bypass nozzle with higher fan pressure ratios, by lower pressure at the core nozzle after the turbine section extracting more work from the flow or by a combination of both effects as has happened in this study. As the turbines pressure ratios gets higher, the outlet temperature of the core gets lower leaving less thermal energy in the flow for evaporation. Therefore, less water can be evaporated which results in lower WARs. This means that the core engine has to become larger and needing more mass flow to produce the required thrust. Since the bypass ratio is constant, this is only possible by an increased fan diameter. Even though the fan pressure ratio increases, the fan diameter increases at a larger scale and thus reducing the specific thrust. Overall this leads to a higher propulsive efficiency and a reduction in specific fuel consumption TSFC. At first the engine gets shorter with higher speed ratios as the condenser is dominating the engines length but the required transfer area becomes smaller due to less water being in the flow. Between speed ratios of 1.0 and 1.05 the condenser is not the main contributor to WET system length as the evaporator and the core engine take over. At this point the overall engine length is no longer determined by the WET system but by the conventional engine components. As the engine gets larger it also gets longer. The engine weighs less with higher speed ratios counter intuitively as the fan diameter increases. On the other hand, the WET system gets continuously lighter as the WAR decreases at the same time and the change of mass in the WET system dominates the overall engine mass. But the impact gets smaller as for higher speed ratios as the curve for engine mass flattens towards higher values until the mass due to increased fan diameter and core engine dominates leading to an overall minimum in engine mass.
Similar to the previous studies, a decrease in water mass flow leads to less heat transfer in the heat exchangers and less power being provided by the steam turbine.

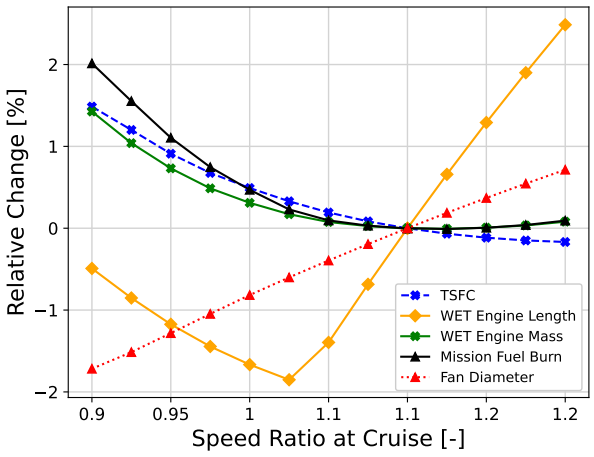

Figure 17 – Mission Fuel Burn

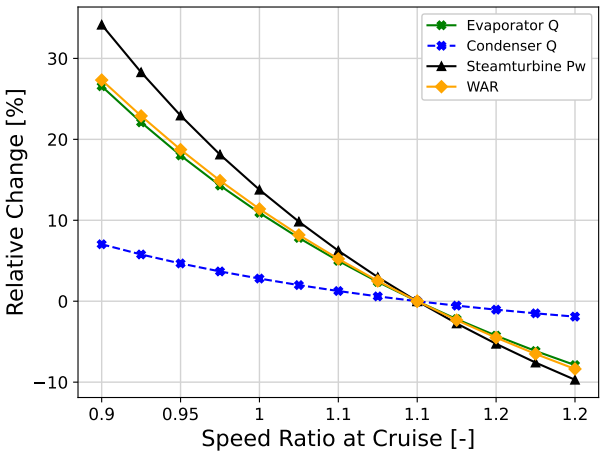

Figure 18 – WET Specifics

5.6 Minimal Temperature Difference for Evaporation

The results of the dT_{min} study are presented in the Figures 19 to 22 for a range of $20\ K < dT_{min} < 55\ K$. The overall difference in mission fuel burn varies with higher dT_{min} from + 0.8 % to - 0.5 %. This value alone has a comparably low impact on mission fuel burn compared to the other conducted studies in this chapter. But it is the main design value for the evaporator defining its size. Although the inlet temperature in the evaporator is almost identical for all study samples, the minimal temperature differences defines the heat transfer of the evaporator and thus the amount of water mass flow that can be evaporated. A larger dT_{min} means less heat transfer and eventually lower WARs. As less water is used to provide the power for thrust generation, more air flow is necessary for the required thrust. This is possible with higher fan diameters. More recuperated heat is beneficial for the thermodynamic cycle and therefore leads to lower TSFC. Due to less heat being transferred for higher dT_{min}, the TSFC increases with this value. The engine length is only affected slightly but a minimum at $dT_{min} = 30K$ is observed. Two opposing trends are responsible for this. The engine diameter increases and so is the core engine but the WET systems become smaller for lower WARs. Those effects are also visible for the engine mass.

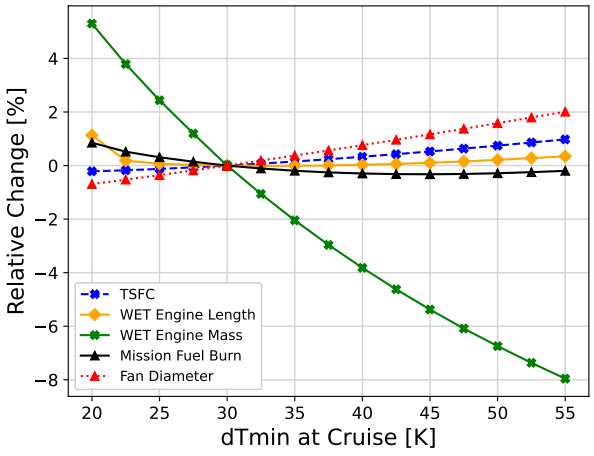

Figure 19 – Mission Fuel Burn

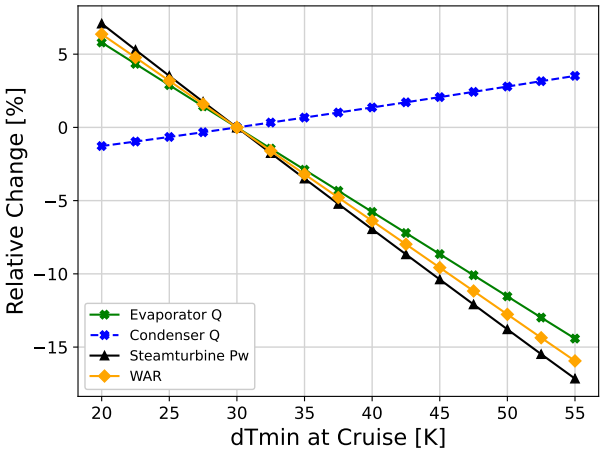

Figure 20 – WET Specifics

As mentioned before, the WAR decreases with higher dT_{min} as there is less heat transferred for evaporation. Similar to the previous studies, this lead to less power provided by the steam turbine. Therefore, the evaporators outlet temperature T_6 gets higher while the condensers outlet temperature T_7 remains almost the same since this temperature is only defined by the amount of water after

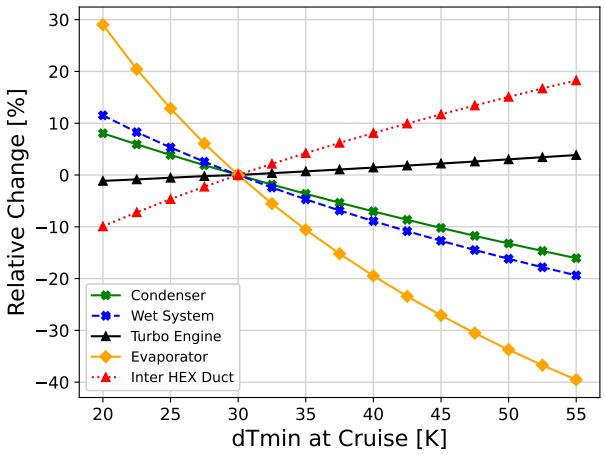

Figure 21 – WET Masses

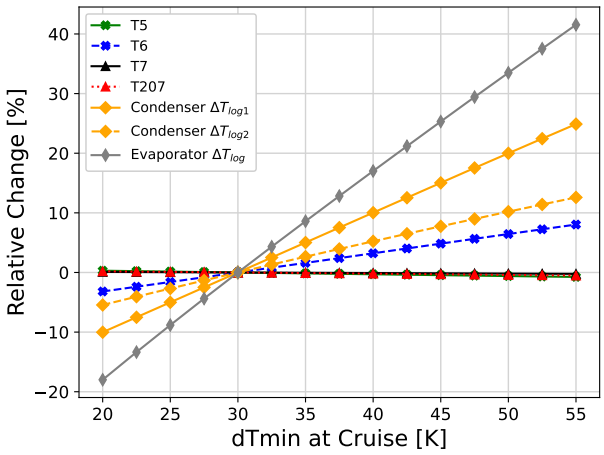

Figure 22 – Temperatures

combustion. Thus, the condenser has to transfer more heat for higher dT_{min}. Although there are different signs for the heat transfer gradients of the heat exchanger, the overall temperature difference between both fluid sides in both heat exchangers grows. Higher temperature differences lead to higher forces for heat transfere and thus less required surface area and weight.

6. Conclusion

In order to investigate the design space and the thermodynamics of the Water-Enhanced Turbofan concept, models for the WET specific components were established. The thermodynamic model and the cycle calculation were combined with geometry generation, mass estimation and turbomachinery efficiency calculation. Those additions were adapted towards the use for a Water-Enhanced Turbofan and its heat exchagers. A iterative design procedure was presented using multiple operating points as input. In addition to the engine design, the aircraft design for an application with a Water-Enhanced Turbofan was presented. This allows to evaluate the engine design not only for thrust specific fuel consumption but also on overall mission fuel burn.
The key findings of this work are the following:

- The overall pressure ratio is strongly limited by the height of the last compressor stage because the core engine becomes small for high pressure levels
- It is beneficial to have higher bypass ratios and larger fan diameters compared to modern conventional turbofan engines
- It is reasonable to operate at comparably low turbine entry temperatures especially because this temperature can be adjusted individually for each operating point
- Nozzle velocity ratios > 1 are contributing to lower mission fuel burn

The entire engine design is heavily dependent on the condenser. Not only because of the heat dissipation from the bypass flow, but also due to the pressure losses generated. In addition, the evaluation at fuel burn level is dominated by the weight and length of the condenser and the evaporator.

7. Copyright Statement

8. Acknowledgments

The research work associated with this publication has been supported by the German Federal Ministry for Economic Affairs and Climate Action under grant number 20M2110B. The funding of the work through the 2nd call of the Federal Aviation Research Program VI (LuFo VI-2), grant project title 'DINA2030plus', is gratefully acknowledged. The authors would like to thank MTU Aero Engines for the close cooperation in the project and the discussions on the Water-Enhanced Turbofan concept.

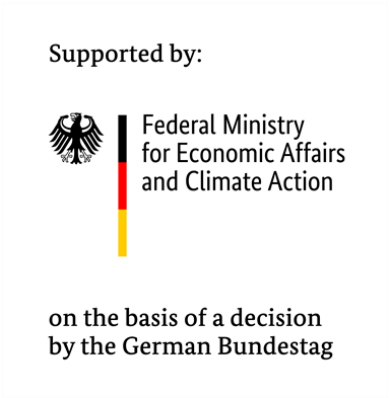

References

[1] European Commission. Fly the green deal: Europe's vision for sustainable aviation. 2022.

[2] Marc Schmelcher and Jannik Häßy. Hydrogen fuel cells for aviation? In *International Society for Air Breathing (ISABE) 2022*, volume 2022.

[3] Oliver Schmitz, Hermann Klingels, and Petra Kufner. Aero engine concepts beyond 2030: Part 1—the steam injecting and recovering aero engine. *Journal of Engineering for Gas Turbines and Power*, 143(2), 2021.

[4] Dah Yu Cheng and Albert L. C. Nelson. The chronological development of the cheng cycle steam injected gas turbine during the past 25 years: Gt-2002-30119. *Journal of Engineering for Gas Turbines and Power*, pages 421–428, 2002.

[5] Alexander Görtz and Björn Schneider. Step-by-step evaluation of the fuel switch from kerosene to hydrogen on the thermodynamic cycle in gas turbine engines: Gt2024-123977. In *ASME Turbo Expo 2024*.

[6] Marc Schmelcher, Jannik Häßy, Alexander Görtz, and Mahmoud El-Soueidan. Methods for the preliminary design of heat exchangers in aircraft engines. In *Proceedings of ASME Turbo Expo 2023: Turbomachinery Technical Conference and Exposition (GT 2023)*, New York, N.Y., 2023. the American Society of Mechanical Engineers.

[7] Marc Schmelcher, Jannik Häßy, Alexander Görtz, Mahmoud El-Soueidan and Fabian Nöske. Integration of heat exchanger models into the performance analysis of innovative aero engine architectures. In *ISABE2024*.

[8] Oliver Schmitz, Sascha Kaiser, Hermann Klingels, Petra Kufner, Martin Obermüller, Martin Henke, Jan Zanger, Felix Grimm, Simon Schuldt, Anna Marcellan, Daniele Cirigliano, Peter Kutne, Alex Heron-Himmel, Stephan Schneider, Judith Richter, Bernhard Weigand, Anne Göhler-Stroh, Arne Seitz, and Mirko Hornung. Aero engine concepts beyond 2030: Part 3—experimental demonstration of technological feasibility. *Journal of Engineering for Gas Turbines and Power*, 143(2), 2021.

[9] Anna Marcellan, Martin Henke, and Simon Schuldt. A numerical investigation of the water-enhanced turbofan laboratory-scale ground demonstrator. In *AIAA SCITECH 2022 Forum*, Reston, Virginia, 2022. American Institute of Aeronautics and Astronautics.

[10] Mahmoud El-Soueidan, Marc Schmelcher, Alexander Gortz, Jannik Hassy, Marius Brocker. Integration of a gas model into cfd analysis for the simulation of turbine exhaust flows with high steam loads. In *Proceedings of ASME Turbo Expo 2023: Turbomachinery Technical Conference and Exposition (GT 2023)*, New York, N.Y., 2023. the American Society of Mechanical Engineers.

[11] Sascha Kaiser, Oliver Schmitz, Paul Ziegler, and Hermann Klingels. The water-enhanced turbofan as enabler for climate-neutral aviation. *Applied Sciences*, 12(23):12431, 2022.

[12] Regina Pouzolz, Oliver Schmitz, and Hermann Klingels. Evaluation of the climate impact reduction potential of the water-enhanced turbofan (wet) concept. *Aerospace*, 8(3):59, 2021.

[13] Bernd Kärcher. Formation and radiative forcing of contrail cirrus. *Nature communications*, 9(1):1824, 2018.

[14] Daniel Silberhorn, Katrin Dahlmann, Alexander Görtz, Florian Linke, Jan Zanger, Bastian Rauch, Torsten Methling, Corina Janzer, and Johannes Hartmann. Climate impact reduction potentials of synthetic kerosene and green hydrogen powered mid-range aircraft concepts. *Applied Sciences*, 12(12):5950, 2022.

[15] Alexander Görtz and Daniel Silberhorn. Thermodynamic potential of turbofan engines with direct combustion of hydrogen. *International Council of the Aeronautical Sciences (ICAS)*, (33rd Congress), 2022.

[16] Alexander Görtz, Jannik Häßy, Marc Schmelcher, and Mahmoud El-Soueidan. Water enhanced turbofan: Improved thermodynamic cycle using hydrogen as fuel: Gt2023-100807. In *Proceedings of ASME Turbo Expo 2023: Turbomachinery Technical Conference and Exposition (GT 2023)*, New York, N.Y., 2023. the American Society of Mechanical Engineers.

[17] Paul Ziegler, Sascha Kaiser, and Volker Gümmer. Parametric cycle studies of the water-enhanced turbofan concept: Gt2023-100529. In *Proceedings of ASME Turbo Expo 2023: Turbomachinery Technical Conference and Exposition (GT 2023)*, New York, N.Y., 2023. the American Society of Mechanical Engineers.

[18] Jannik Häßy, Alexander Görtz, Marc Schmelcher, Jens Schmeink, and Mahmoud El-Soueidan. On the water enhanced turbfan concept: Part b - flow path and mass assessment. In *34th Congress of the International Council of the Aeronautical Sciences 2024 (ICAS)*.

[19] M. Lüdemann. Blade: A modular environment for traceable and automated aircraft design. In *Proceedings of the 13th EASN International Conference 2023*, Salerno, Italy, 2023.

[20] D. Raymer. *Aircraft Design: A Conceptual Approach*. The American Institute of Aeronautics and Astronautics (AIAA), Washington, DC, USA, 6th edition, 2018.

[21] Airbus Customer Service. Getting to grips with aircraft performance, 2002.

[22] E. Torenbeek. *Advanced Aircraft Design: Conceptual Design, Analysis, and Optimization of Subsonic Civil Airplanes*. John Wiley & Sons, Chichester, UK, 2013.

[23] Deutsches Zentrum für Luft- und Raumfahrt. Cpacs: A common language for aircraft design.

[24] David L. Daggett. Water injection feasibility for boeing 747 aircraft.

[25] Stanislaus Reitenbach, Alexander Krumme, Thomas Behrendt, Markus Schnös, Thomas Schmidt, Sandrine Hönig, Robert Mischke, and Erwin Mörland. Design and application of a multidisciplinary predesign process for novel engine concepts. *Journal of Engineering for Gas Turbines and Power*, 141(1), 2019.

[26] Jannik Häßy and Jens Schmeink. Knowledge-based conceptual design methods for geometry and mass estimation of rubber aero engines. *ICAS*, 2022.

[27] Jannik Häßy, Martin Bolemant, and Richard-Gregor Becker. An educated guess - predicting turbomachinery efficiencies of aero engines during conceptual design. In *Proceedings of ASME Turbo Expo 2023: Turbomachinery Technical Conference and Exposition (GT 2023)*, New York, N.Y., 2023. the American Society of Mechanical Engineers.

[28] Richard Becker, Florian Wolters, Mobin Nauroz, and Tom Otten. Development of a gas turbine performance code and its application to preliminary engine design. *Deutscher Luft- und Raumfahrtkongress DLRK*, 2011.

[29] Abhijit Guha. Optimum fan pressure ratio for bypass engines with separate or mixed exhaust streams. *Journal of Propulsion and Power*, 17(5):1117–1122, 2001.

[30] Hubert Grieb, editor. *Projektierung von Turboflugtriebwerken*. Technik der Turboflugtriebwerke. Birkhäuser Basel, Basel and s.l., 2004.

[31] Fabian Nöske. Modellierung und bewertung des off-design verhaltens von verdampfern in der triebwerksvorauslegung. In *Technical University of Berlin*.

[32] *VDI-Wärmeatlas*. SpringerLink Bücher. Springer Vieweg, Berlin, Heidelberg, 11., bearb. und erw. aufl. edition, 2013.

[33] J. R. García-Cascales, F. Vera-García, J. M. Corberán-Salvador, and J. Gonzálvez-Maciá. Assessment of boiling and condensation heat transfer correlations in the modelling of plate heat exchangers. *International Journal of Refrigeration*, 30(6):1029–1041, 2007.